[Chem. Pharm. Bull. 34(11)4457—4466(1986)]

Quantum-Chemical Elucidation of the Mechanism of the NIH-Shift during Aryl Hydroxylation Catalyzed by Cytochrome P-450

MINORU TSUDA,* SETSUKO OIKAWA, YORIKO OKAMURA, KATSUHIKO KIMURA, TADASHI URABE and MITSUO NAKAJIMA

Faculty of Pharmaceutical Sciences, Chiba University, 1–33, Yayoi-cho, Chiba 260, Japan

(Received March 24, 1986)

The ring substituent dependence in the NIH-shift (the migration of a hydrogen atom during aryl hydroxylation catalyzed by cytochrome P-450) was investigated by semi-empirical molecular orbital calculations. The lowest energy path, the intrinsic reaction coordinate, was found on the $3N-6$ dimensional potential energy hypersurface of the protonated arene oxide ring opening (aniline and acetanilide were selected as substrates of class I, and benzene and anisole as substrates of class II). The conclusions are as follows: a) The NIH-shift occurs by a simple and common mechanism regardless of class I or class II categorization; *i.e.*, the Meisenheimer-type intermediate having a *para*-quinoid structure spontaneously produced from the protonated arene oxide passes over the saddle point of hydrogen migration to an adjacent position of the aromatic ring. b) The theoretically obtained reaction rate constants reproduce quantitatively the experimental data on the retention of deuterium, on the assumption that the deuterium retention is determined by the rate constant reflecting the potential energy barrier height from the Meisenheimer-type tetrahedral intermediate to the final product. This result may suggest that the P-450-catalyzed 4-hydroxylation of aromatics involves a tetrahedral intermediate as the first product with the absence of epoxide formation.

Keywords——cytochrome P-450; hydroxylation; NIH-shift; intrinsic reaction coordinate; MINDO/3; molecular orbital method; Meisenheimer-type intermediate; tetrahedral intermediate; epoxide

The NIH-shift is a characteristic of the oxidation of aromatic compounds catalyzed by cytochrome P-450, a widely distributed mono-oxygenase.[1] Recent development in the biomimetic chemistry of artificial model systems[2] of P-450 have led to renewed interest in the mechanism of the NIH-shift, which is one of the criteria for the evaluation of model systems.

Pudzianowski *et al.* made molecular orbital (MO) calculations on the oxidation mechanisms of methane and ethylene[3] as well as CCl_4 and $CHCl_3$[4] by singlet and triplet oxygen atoms as a model of P-450 oxidation. An MO study was carried out in this laboratory[5] by another method on the oxidation of benzene by a singlet oxygen atom as a model of the oxygenated heme intermediate, Fe^{III}–O or $Fe^{V}=O$, which is the ultimate species in P-450 oxidation. The intrinsic reaction coordinate (IRC) following the oxidation reaction path on the $3N-6$ dimensional potential energy hypersurface (N is the number of atoms of the reaction system) leads to epoxide formation spontaneously.

Burka *et al.*[6] proposed a more detailed mechanism for the reaction of $Fe^{V}=O$ with halobenzenes, where $Fe^{V}=O$ oxidizes the substrate to produce an aromatic radical cation and then changes to $Fe^{IV}=O$ having radical character. These products combine to the selective formation of a *meta*-substituted tetrahedral cationic intermediate. *ortho*- and *para*-hydroxylated halobenzenes would arise from rearrangement of the 2,3- and 3,4- areneoxide produced by ring closure of the *meta*-substituted cationic intermediate.

The enzymatic hydroxylation of specifically tritiated and deuterated aromatic substrates

is accompanied with migration of the heavy isotope from the site of hydroxylation to an adjacent position in the aromatic ring (the NIH-shift): *i.e.*, a high migration corresponds to a high retention of the label isotope. The NIH-shift is also observed in the acid-catalyzed isomerization of 1-^{2}H-4-methylbenzene oxide[7] and 1-^{2}H-naphthalene oxide[8] to the corresponding phenols. Thus the NIH-shift occurs even without the help of P-450.

The IRC of the NIH-shift of benzene oxide has already been investigated[5] and the result is shown in Fig. 2(a) of this paper. Ferrell and Loew also made a mechanistic study of the acid-catalyzed rearrangement of benzene oxide by means of MINDO/3 calculations, and the result suggested that the reaction involves rate-determining S_N1 type formation of a carbocation, quickly followed by the NIH-shift.[9]

In the present paper, the IRC study of the NIH-shift was extended to examine the ring substituent dependence of the migration of the hydrogen atom during aryl hydroxylation by P-450. The $3N-6$ dimensional potential energy hypersurface of the NIH shift was investigated in detail along the lowest energy path (IRC path) of the reaction, with aniline and acetanilide as substrates of class I and benzene and anisole as substrates of class II. In the NIH-shift mechanism postulated by Daly *et al.*[10] and described in textbooks and review papers,[11] a neutral 2,5-cyclohexadienoid intermediate plays an important role; it can be formed if the substrate contains a substituent capable of undergoing ionization. Substrates were divided into class I and class II, on the basis that compounds of class I but not those of class II can produce such an intermediate. The IRC study quantitatively reproduced the experimental values of the percent retention of deuterium for every investigated compounds, regardless of class I and class II categorization.

Method

A mass-weighted Cartesian coordinate was adopted in the construction of the $3N-6$ dimensional potential energy hypersurface. The structure of a stable molecule is located at a potential energy minimum having $3N-6$ normal modes of vibration of real frequency. The structure of an activated complex at the transition state of a reaction exists at the saddle point having a unique normal mode of vibration of imaginary frequency as well as the $3N-7$ normal modes of vibration of real frequency. The IRC is defined as the steepest descent path starting from a saddle point toward both the plus and minus directions of the imaginary vibration.[12] Obviously, the IRC is the lowest energy path among many possible reaction coordinates.

In the calculation of the adiabatic potential energy, MINDO/3[13] parametrization was adopted considering all the valence electrons. *Ab initio* restricted Hartree Fock (RHF) MO calculations with the MINI basis set were also carried out in order to confirm the reliability of the present MINDO/3 calculations, where MINI-1 was used for hydrogen and carbon atoms and MINI-2 for oxygen atom. MINI-1 and MINI-2 are a minimal-type basis set proposed by Tatewaki and Huzinaga.[14] Linear combinations of three primitive Gaussian-type functions are used for 1*s*, 2*s* and 2*p* atomic orbitals in MINI-1 and 1*s* and 2*s* in MINI-2, whereas 2*p* in MINI-2 is expressed with four Gaussians.

The method of finding a minimum and a saddle point on the multidimensional hypersurface was reported in detail elsewhere.[15] The vibrational analysis[16] was carried out at these fully optimized stationary points in terms of the harmonic vibrational frequencies, and the results obtained were used for the calculations of molecular partition functions related to the thermodynamic functions.[17] The programs for these calculations were written by us,[15] except for *ab initio* calculation, which done with IMSPAK, a Library Program of the Institute for Molecular Science, Okazaki, Japan.

Results

IRC Path of the NIH-Shift

The qualitative potential energy changes along the IRC paths of protonated arene oxides are collected in Fig. 1 for the NIH shift of benzene, aniline, acetanilide and anisole in the P-450-catalyzed hydroxylation process. The characteristic feature is that the 4-hydroxylation process starting from the epoxide ring opening gives the same type of potential energy change irrespective of class I or class II categorization, strongly suggesting that the classification is

meaningless. The protonated arene oxide (A) produces an intermediate (C_P) at first and then passes over the saddle point (D_P) for the shift of the hydrogen atom to the adjacent position (Figs. 1—5). There is a small peak of the saddle point (B_P) for the intermediate (C_P) formation from the protonated arene oxide (A) for both acetanilide (class I) and anisole (calss II), but no saddle point substantially in the case of aniline (class I), where the protonated arene oxide (A) spontaneously produces the Meisenheimer-type intermediate (C_P).

Protonated benzene oxide shows quite different behavior from these three cases of 4-hydroxylation, where the epoxide ring opening process from A to C requires much activation energy and the shift of a hydrogen atom from the intermediate C to the product E takes place easily, passing over a small peak of the saddle point D (Fig. 2(a)). The same characteristic is observed in the case of 3-hydroxylation of aniline (Fig. 3(a)). These results mean that the Meisenheimer-type intermediate is unstable in the cases where no substituent exists a at the *para*-position of an aromatic ring. When the potential energy changes of Fig. 1 are examined, it is clear that 3-hydroxylation is prohibited in the P-450 enzymatic oxidation of mono-substituted benzenes, and 4-hydroxylation is predominant, provided that an arene oxide is the precursor.

Prior to further discussion, let us examine the reliability of the present potential energy values calculated by MINDO/3. *Ab initio* calculations on the ring opening reaction of a protonated ethylene oxide with various basis sets have been carried out by many authors[18,19] although there has been no calculation on benzeneoxide. A summary of the *ab initio* calculations on ethylene oxide is shown in Table I for comparison with the results of MINDO/3. In the RHF calculations, the improvement of the basis set from STO-3G to Dunning's[19] reduces the heat of formation and the activation energy monotonously, except the 6-31 G** basis set. However, the electron correlation incorporated at the levels of the second (MP2) and the third (MP3) order Möller–Plesset perturbation theory increases the values again. The improvement with both the basis set (6-31 G**) and the electron correlation (MP2) gives 24.78 kcal/mol for the heat of formation and 35.34 kcal/mol for the activation energy of ring opening. These best values are in good agreement with the results

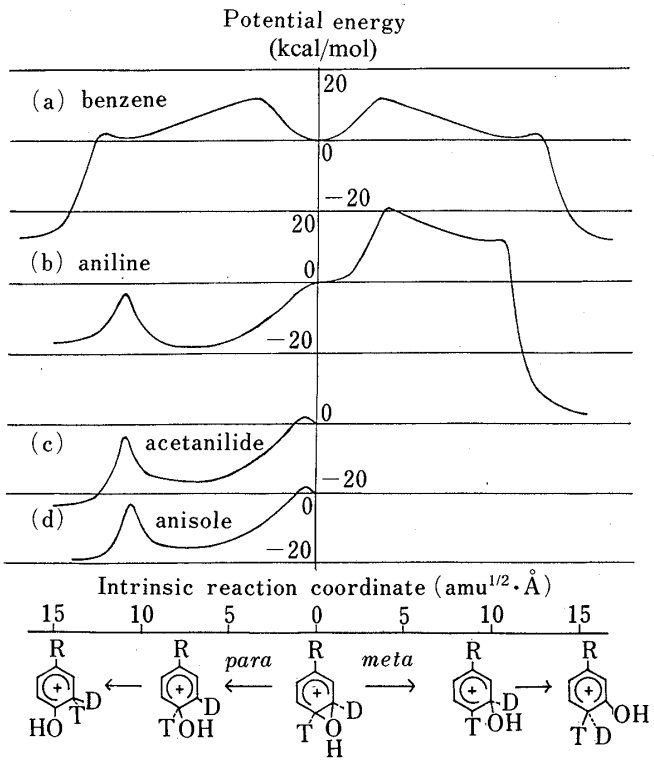

Fig. 1. Collection of Qualitative Potential Energy Curves along the Intrinsic Reaction Coordinate of NIH-Shift of Protonated Arene Oxides
(a) benzene (b) aniline (c) acetanilide (d) anisole.

TABLE I. Relative Energies of the Ring-Opening Reaction of a Protonated Ethylene Oxide[a]

Basis set	Heat of formation (kcal/mol)	Activation energy (kcal/mol)
STO-3G[b]	41.11	47.21
MINI[d]	13.42	—
4-31G[b]	9.63	16.79
6-31G//4-31G[b]	8.96	16.07
6-31G**//4-31G[b]	11.58	20.21
Dunning's[c]	7.2	—
MP2/6-31G//4-31G[b]	21.18	29.68
MP3/6-31G//4-31G[b]	18.33	26.74
MP2/6-31G**//4-31G[b]	24.78	35.34
MINDO/3[d]	24.52	33.20

a) All the energies are obtained from the fully optimized geometry with each basis set and are measured from an epoxide as a standard. *b*) Cited from ref. 15. The notation "MP3/6-31G**//4-31G," for example, means a third-order Möller–Plesset calculation with the 6-31G** basis set (6-31G plus a set of *d* type functions (5*d*) on carbon and oxygen atoms and a set of *p* type functions on hydrogen atom) on the structure fully optimized by the 4-31G basis set. *c*) Cited from ref. 16. *d*) This work.

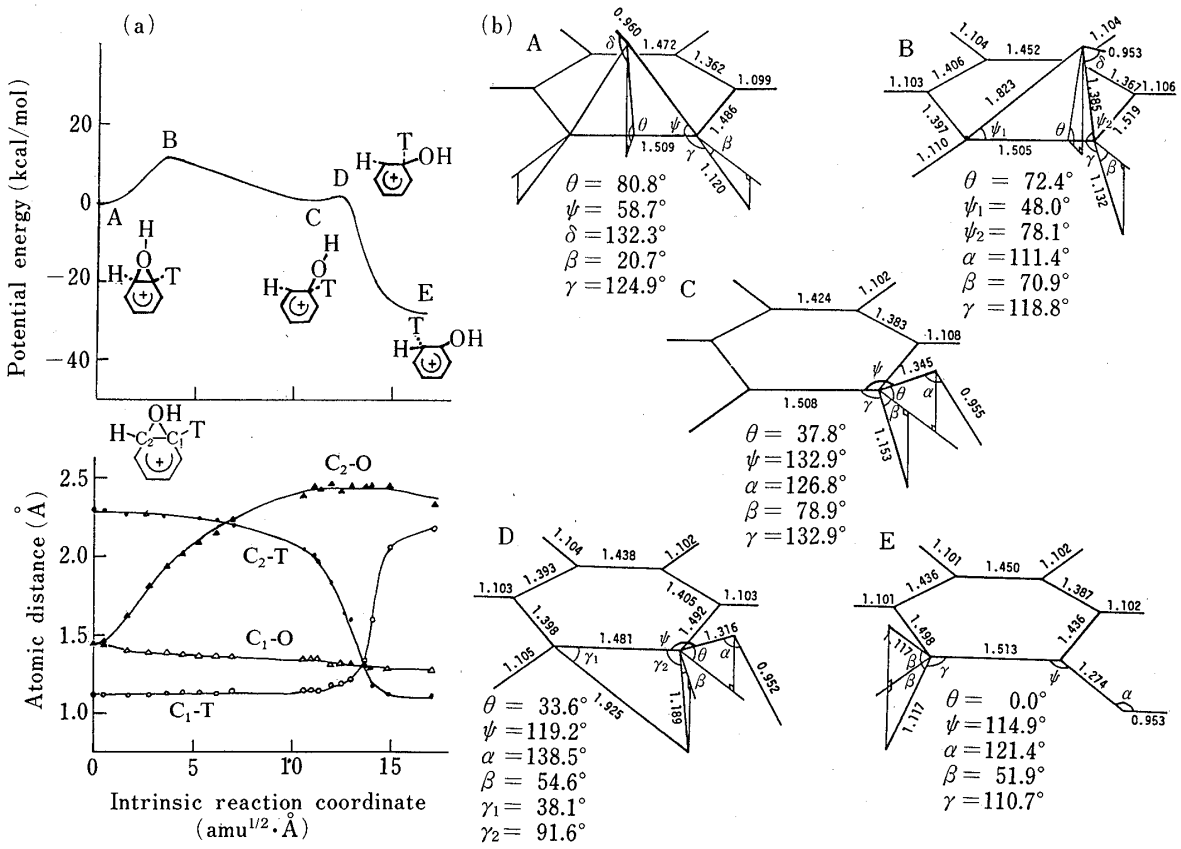

Fig. 2(a). The Detailed Potential Energy Change Along the IRC together with Several Kinds of Atomic Distance Changes in the Case of Benzene

Fig. 2(b). Optimized Structures at the Stationary Points on the IRC in the Case of Benzene

A, the starting protonated species; B, the saddle point for the ring opening; C, the Meisenheimer-type intermediate; D, the saddle point for hydrogen migration (NIH-shift); E, the final product on the route of hydroxylation. A and B have the Cs symmetry.

obtained by MINDO/3.

Reaction System Structures and Their Changes through the Reaction Path

A complete understanding of the reaction mechanism involves knowing the exact position of every atom in the molecular system during the reaction.[20] The present IRC calculation can reveal the positions of all atoms in the reacting molecule and their displacements throughout the reaction path. Figures 2(a), 3(a), 4(a) and 5(a) show the detailed potential energy change along the IRC together with several examples of the atomic distance changes in the cases of benzene, aniline, acetanilide and anisole, respectively. The NIH-shift proceeds in two steps: *i.e.*, a ring opening to form a Meisenheimer-type intermediate in the first step and a hydrogen atom migration in the second step. The chemical structures at the stationary points on the IRC are shown in Figs. 2(b), 3(b), 4(b) and 5(b): *i.e.*, the starting protonated species, A, the saddle point for the ring opening, B, the Meisenheimer-type intermediate, C, the saddle point for hydrogen migration (the NIH-shift), D, and the final product, E. The suffix M or P is added for the route of 3- or 4-hydroxylation, respectively. From the structures at the stationary points in Figs. 2(b), 3(b), 4(b) and 5(b), and the bond distance changes following the IRC route in Figs. 2(a), 3(a), 4(a) and 5(a), one can visualize the reaction mechanism of the NIH-shift in detail.

More realistic displays are presented in Fig. 6(a) and 6(b), which are serial snap-shots of atomic migrations during the NIH-shift of aniline. In the first step, the ring-opening proceeds as if the epoxide oxygen is pulled by a hydrogen atom to form hydroxyl group at the *para*-position. At the same time, the hydrogen atoms binding the C_4 and C_3 atoms move down and up, respectively, to form the Meisenheimer-type intermediate, C_P, as shown in Fig. 6(a). In the second step, as shown in Fig. 6(b), the hydrogen atom bound to the C_4 atom moves to form a triangle structure of the saddle point, D_P (filled circles), where the hydrogen binds to both the C_3 and C_4 atoms. The characteristic feature observed in Fig. 6(b) is that the hydrogen atom

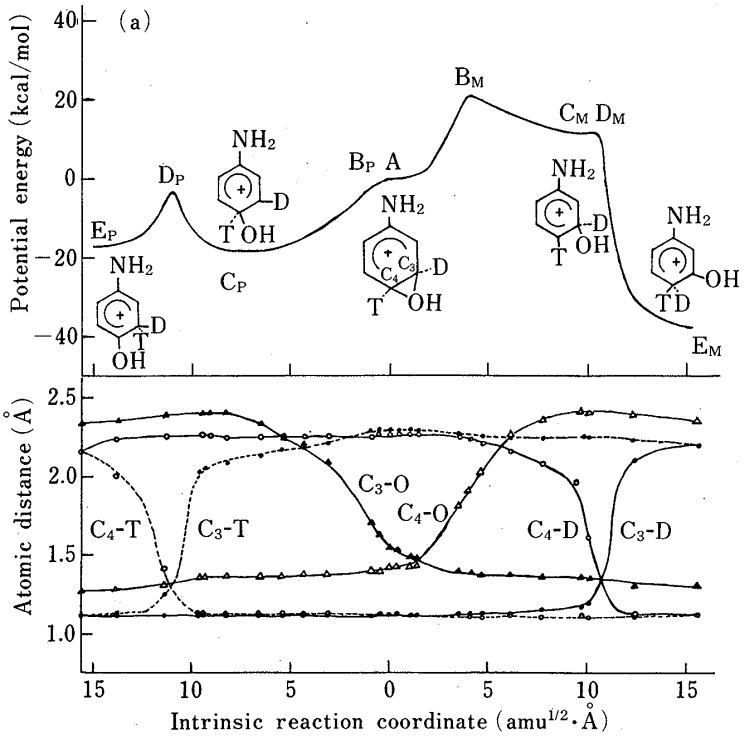

Fig. 3(a). The Detailed Potential Energy Change along the IRC together with Several Examples of Atomic Distance Changes in the Case of Aniline

B_P has the same energy as A in this case.

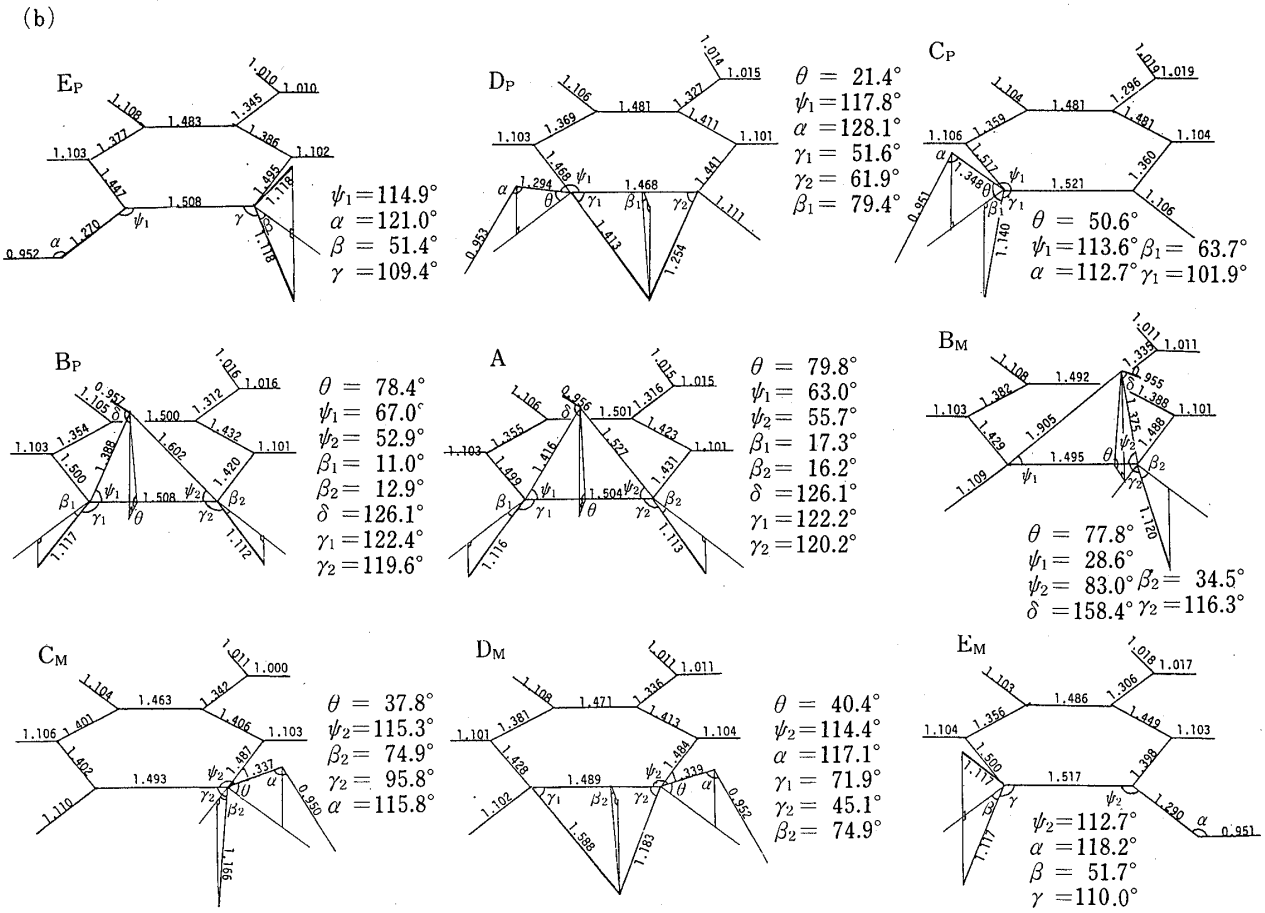

Fig. 3(b). Optimized Structures at the Stationary Points on the IRC in the Case of Aniline

See Fig. 2(b) for the notation of the structure. The suffix P or M shows the 4- or 3-hydroxylation process, respectively.

which migrates from C_4 to C_3, keeps a constant distance from the C_3–C_4 bond and a constant angle to the molecular plane, although these atomic displacements following the IRC route give the average image of structural change of the reacting molecule. In spite of the entirely different characteristic in the potential energy change, the atomic displacements in 3-hydroxylation are analogous to those in 4-hydroxylation; *i.e.*, displacements analogous to those of Figs. 6(a) and 6(b) were observed in the case of 3-hydroxylation of aniline.

The Meisenheimer-type intermediates C_P (Figs. 3(b), 4(b) and 5(b)) have a quinoid structure, where the C_2–C_3 and C_5–C_6 bonds have the length of 1.36 Å, nearly equal to the corresponding bonds of *p*-benzoquinone (1.344 Å). The *para*-quinoid structure is the origin of the stability of the intermediate C_P in 4-hydroxylation whereas the unstable intermediate C_M in 3-hydroxylation has no quinoid structure. For this reason the predominance of 4-hydroxylation and the inhibition of 3-hydroxylation are observed (Fig. 3(a)). Once an arene oxide has been produced by direct epoxidation or by epoxide ring closure,[5] 4-hydroxylation takes place exclusively and no 3-hydroxylation is observed in this case. Daly *et al.*[10] proposed that *ortho*-quinoid structure formation is the motive force of the NIH-shift (class II), and *para*-quinoid formation lowers the yield of the NIH-shift in 4-hydroxylation (class I). This mechanism has been cited in many books.[11,21] It should be noted, however, that a *para*-quinoid intermediate C_P is always produced in 4-hydroxylation regardless of class I [aniline (Fig. 3(a)) and acetanilide (Fig. 4(a))] or class II [benzene (Fig. 2(a)) and anisole (Fig. 5(a))] categorization.

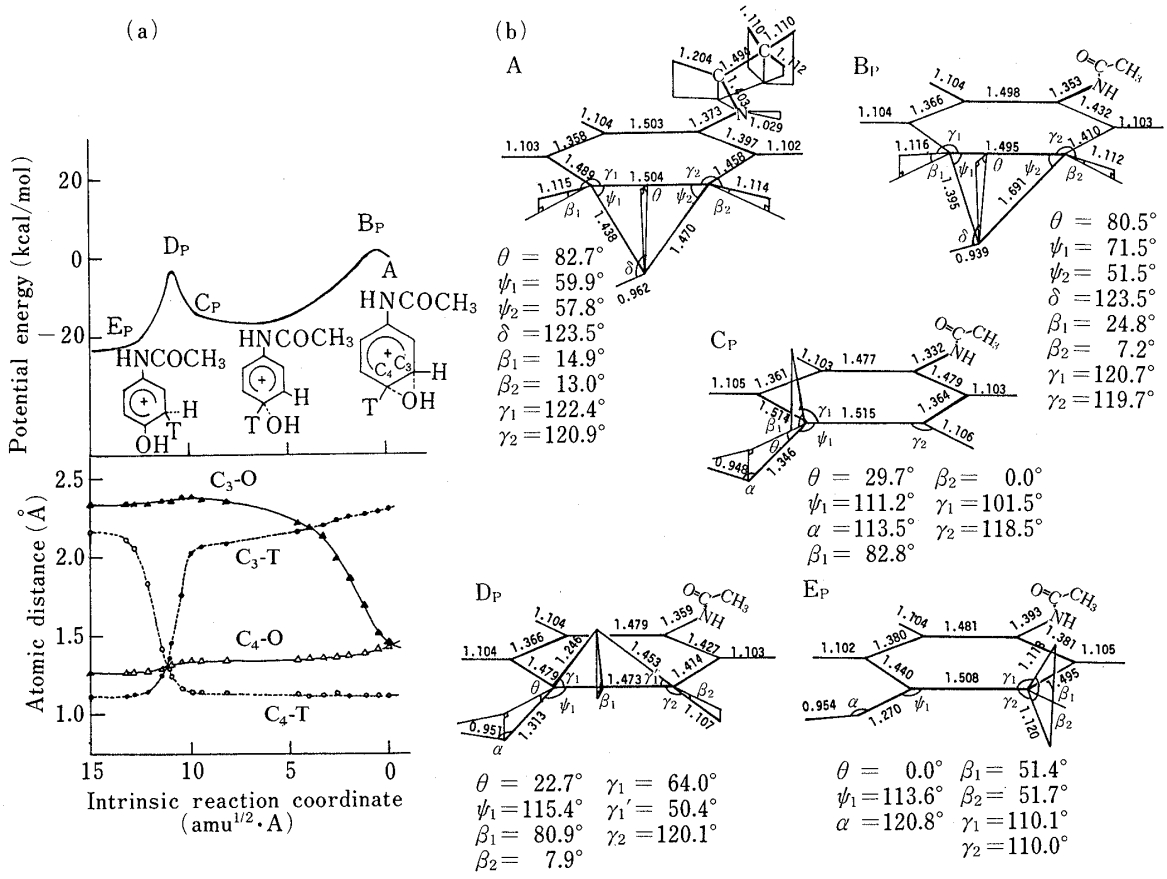

Fig. 4(a). The Detailed Potential Energy Change along the IRC together with Several Examples of Atomic Distance Changes in the Case of Acetanilide

Fig. 4(b). Optimized Structures at the Stationary Points on the IRC in the Case of Acetanilide

See Fig. 2(b) for the notation of the structure. The suffix P means the 4-hydroxylation process.

Reaction Mechanism of the NIH-Shift

Reaction Rate Constant——Provided that the reactions shown in Figs. 3, 4 and 5 take place in one step immediately after the arene oxides are protonated, the NIH-shift will be observed in high yield in all 4-hydroxylations regardless of class I or class II categorization, because no activation energy is required for the aniline case and only small activation energies for the acetanilide and anisole cases at the first saddle point B_P. Moreover, the potential energy of the second saddle point D_P is lower than that of the first saddle point B_P in every case. However, the experiment by Daly *et al.* shows that 4-hydroxyaniline formed from aniline-4-D retains only 6% of the deuterium. 4-Hydroxyacetanilide from acetanilide-4-D and 4-hydroxyanisole from anisole-4-D retained 30% and 60% of the deuterium, respectively.[10] These experiments suggest that excess kinetic energy is lost in the medium during the ring-opening reaction and the NIH-shift reaction restarts from the intermediate C_P which passes over the saddle point D_P to produce E_P; *i.e.*, the tetrahedral intermediate C_P in enzymatic hydroxylation by P-450 is strongly restricted in the enzyme pocket, different from the case in usual organic reactions. In this situation, the experimental value of the percent retention of deuterium is proportional to the reaction rate passing over the saddle point D_P, since the experiment measured less than 20% substrate conversion in the initial period of liver microsome hydroxylation[10] and furthermore the product E_P is removed to yield the final

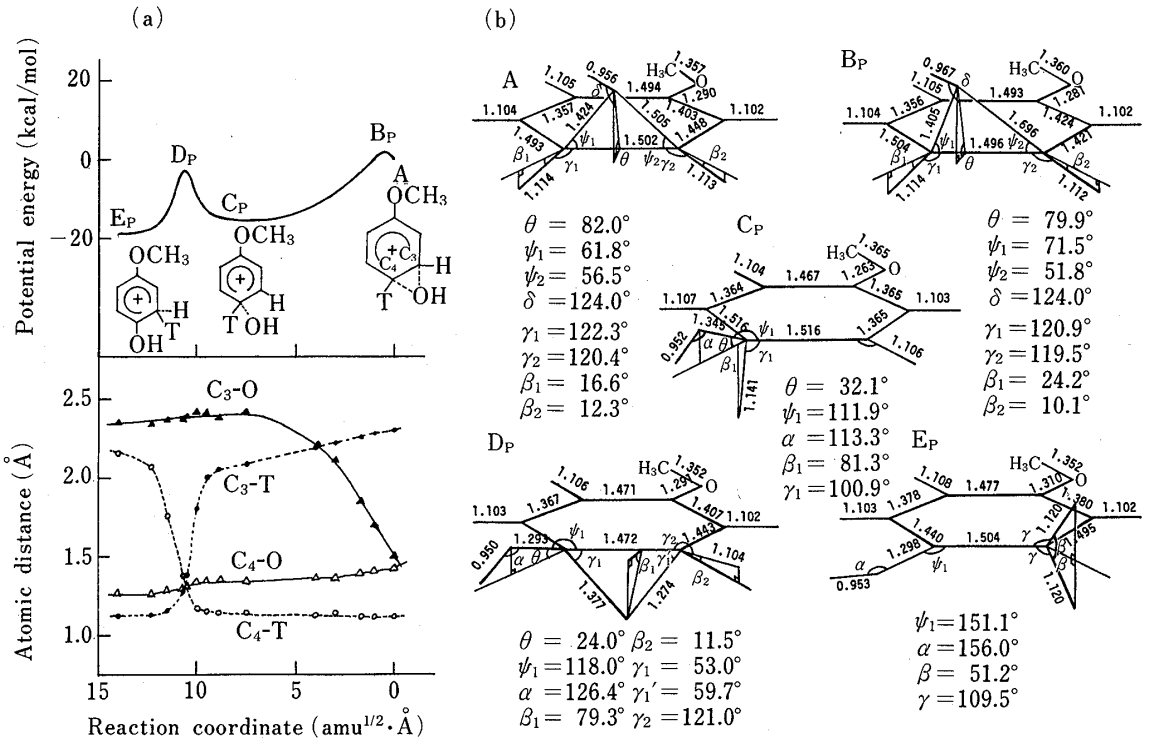

Fig. 5(a). The Detailed Potential Energy Change along the IRC together with Several Examples of Atomic Distance Changes in the Case of Anisole

Fig. 5(b). Optimized Structures at the Stationary Points on the IRC in the Case of Anisole

See Fig. 2(b) for the notation of the structure. The suffix P means the 4-hydroxylation process.

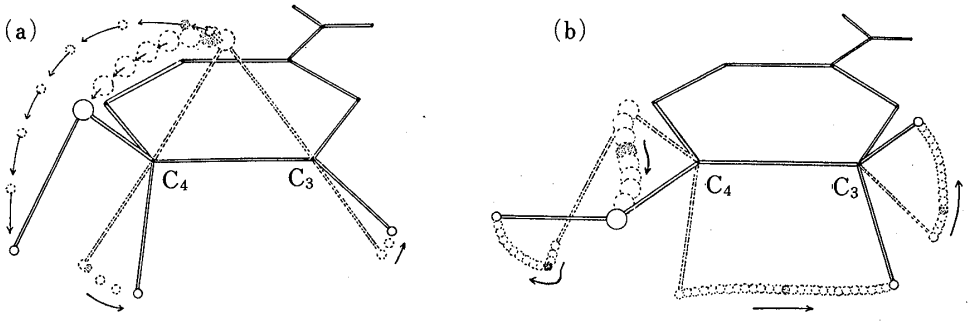

Fig. 6. Serial Snap-Shots of Atomic Migrations along the IRC in the Case of Aniline

(a) ring opening starting from A, passing over B shown by ◎, to P. (b) hydrogen migration (NIH-shift), starting from P, passing over D shown by ◎, to E.

product of oxidation, a phenol derivative.

The reaction rate constant $k(T)$ is given theoretically by Eq. 1 when Eyring's transition state theory is adopted[17]:

$$k(T)=\kappa(\boldsymbol{k}T/\boldsymbol{h})(Q^{*}/Q)\exp(-\Delta E^{\circ *}/\boldsymbol{N}\boldsymbol{k}T) \quad (1)$$

where κ is the transmission coefficient, $\boldsymbol{k}$ Boltzmann constant, T the reaction temperature, $\boldsymbol{h}$ Plank constant, $\boldsymbol{N}$ Avogadro number, Q^{*} molecular partition function of the activated com-

TABLE II. The Rate Constant and the Equilibrium Constant in the NIH-Shift Reaction

	$\Delta E^{\circ\ddagger}$ a) (kcal/mol) and [k]d)	$\Delta F^{\circ\ddagger}$ (kcal/mol) and [k]d)	Exp.b) (%) and [Ratio]	ΔE° a) (kcal/mol)	ΔF° (kcal/mol)	Kc) and [Ratio]
Aniline (*para*)	13.83 [0.022]	14.10 [0.117]	6 [0.1]	0.31	−0.09	1.16 [0.003]
Acetanilide	12.15 [0.337]	12.54 [0.387]	30 [0.5]	−7.10	−7.06	$9.45\cdot10^4$ [245]
Anisole	11.48 [1]	11.95 [1]	60 [1]	−3.78	−3.67	$3.86\cdot10^2$ [1]

a) $\Delta E^{\circ\ddagger}$ and ΔE° include the zero-point energy. b) The deuterium retention (%) in the 4-hydroxylation cited from ref. 8. c) K: The equilibrium constant at 310 K (37 °C). d) k: The relative rate constant at 310 K. The rate constant of anisole is taken as unity as a standard.

plex at the saddle point D_P, Q molecular partition function of the intermediate C_P, $\Delta E^{\circ\ddagger}$ the activation energy in the reaction from the intermediate C_P to the product E. Since there will be no volume change following the NIH-shift in liver microsome hydroxylation ($\Delta V=0$), the Eq. 1 is applicable for the calculation in the rate constant in the present cases, because the molar standard Gibbs function change ΔG° is reduced to the standard Helmholz function change ΔF°. From the Eq. 1,

$$\ln k(T)=\ln\kappa(\boldsymbol{k}T/\boldsymbol{h})-\Delta F^{\circ\ddagger}/\boldsymbol{N}\boldsymbol{k}T \qquad (2)$$

$$\Delta F^{\circ\ddagger}=(\Delta E^{\circ\ddagger}-\boldsymbol{N}\boldsymbol{k}T\ln Q^{\ddagger})+\boldsymbol{N}\boldsymbol{k}T\ln Q$$

Although Q contains $Q_{\text{translation}}$, Q_{rotation} and $Q_{\text{vibration}}$, the contributions from the translation and the rotation were excluded in the calculation of molecular partition function, because the reaction takes place in the enzyme pocket in the present case. Thus $\Delta F^{\circ\ddagger}$ can be calculated from the potential energy difference between D_P and C_P, $\Delta E^{\circ\ddagger}$, and the vibrational molecular partition function $Q^{\ddagger}$ and Q which is evaluated from the vibrational frequencies of normal modes obtained by vibration analysis at D_P and C_P. The values of $\Delta F^{\circ\ddagger}$ and the relative rate constants at 37 °C calculated by using Eqs. 1 and 2 are collected in Table II, where the rate constant in the anisole case was postulated to be unity as a standard. We checked that the relative rate constants in Table II are scarcely modified by the addition of the contribution of rotation. Rough estimation of the rate constant was done by using only the activation $\Delta E^{\circ\ddagger}$ excluding the activation entropy term (Table II). However, a more precise calculation using $\Delta F^{\circ\ddagger}$ gives better agreement with the experiment. This suggests the importance of the entropy term.

Equilibrium Constant——Another possible factor determining the experimental deuterium retention ratio is the equilibrium constant K between C_P and E_P. The K was calculated by using Eq. 3.

$$K(T)=\exp(-\Delta F^{\circ}/\boldsymbol{N}\boldsymbol{k}T) \qquad (3)$$

$$\Delta F^{\circ}=\Delta E^{\circ}+\boldsymbol{N}\boldsymbol{k}T(\ln Q_1-\ln Q_2)$$

where Q_1 and Q_2 are the partition functions of E_P and C_P, respectively, and ΔE° is the energy difference between E_P and C_P. Unfortunately, none of the equilibrium constants obtained here are consistent with the experiments (Table II). This result is reasonable, because Daly *et al.*'s experiments[10] are those on the initial period of liver microsome hydroxylation.

Reaction Mechanism——Starting from an arene oxide produced by direct oxidation of the π-electron system or ring closure of the tetrahedral intermediate, the lowest energy path on

the potential energy hypersurface of the NIH-shift and the structure change of the reaction system following this path were elucidated in the cases of benzene, aniline, acetanilide and anisole. As shown in Fig. 2, 3, 4 and 5, the mechanism is simple and common to all cases, regardless of class I or class II categorization.

Theoretical calculation reproduced the experimental data well as shown in Table II on the assumption that the yield of the NIH-shift is determined by the reaction rate constant $k(T)$ from the tetrahedral *para*-quinoid type intermediate C_P passing over the saddle point D_P to the final product E_P, where the main contribution to the rate constant is the activation energy $\Delta E^{\circ\neq}$ (the peak height of D_P measured from C_P) although the activation entropy term is also important. This result may support another mechanism recently proposed by Bush and Trager,[22] that the tetrahedral intermediate C_P is the first product in the absence of epoxide formation in 4-hydroxylation of aromatics catalyzed by cytochrome P-450. Research on this point is in progress.

Acknowledgement The authors thank the Computer Center, Institute for Molecular Science, Okazaki, for the use of a M-200H computer and the Library program IMSPAK in *ab initio* calculations. The computations were mainly carried out at the Computer Center, the University of Tokyo, and the Computer Center, Chiba University.

References and Notes

1) O. Hayaishi, "Molecular Mechanisms of Oxygen Activation," Academic Press, New York, 1974.
2) *a*) J. T. Groves, T. E. Nemo and R. S. Myers, *J. Am. Chem. Soc.*, **101**, 1032 (1979); *b*) T. A. Hinrichs, V. Ramachandran and R. W. Murray, *ibid.*, **101**, 1282 (1979); *c*) I. Tabushi and N. Koga, *ibid.*, **101**, 6456 (1979); *d*) J. T. Groves and W. J. Kruper, Jr., *ibid.*, **101**, 7613 (1979); *e*) J. T. Groves, R. C. Haushalter, M. Nakamura, T. E. Nemo and B. J. Evans, *ibid.*, **103**, 2884 (1981); *f*) H. J. Ledon, P. Durbut and F. Varescon, *ibid.*, **103**, 3601 (1981); *g*) T. A. Dix and L. J. Marnett, *ibid.*, **103**, 6744 (1981); *h*) I. Tabushi and A. Yazaki, *ibid.*, **103**, 7371 (1981); *i*) M. W. Nee and T. C. Bruice, *ibid.*, **104**, 6123 (1982); *j*) S. Ito, K. Inoue and M. Matsumoto, *ibid.*, **104**, 6450 (1982); *k*) J. A. Smegel and C. L. Hill, *ibid.*, **105**, 2920 (1983).
3) A. T. Pudzianowski and G. H. Loew, *J. Am. Chem. Soc.*, **102**, 5443 (1980).
4) A. T. Pudzianowski, G. H. Loew, B. A. Mico, R. V. Branchflower and L. R. Pohl, *J. Am. Chem. Soc.*, **105**, 3434 (1983).
5) M. Tsuda, S. Oikawa and K. Kimura, Abstract of 3rd Int'l Quantum Chem., Kyoto, 1979, p. 30-V-7; for the IRC studies of organic molecules by a singlet oxygen atom, see M. Tsuda, S. Oikawa, S. Ohnogi and A. Suzuki, "ME-80," ed. by R. P. Kramer, Delft Univ. Press, Amsterdam, 1980, p. 553.
6) L. T. Burka, T. M. Plucinski and T. L. MacDonald, *Proc. Natl. Acad. Sci. U.S.A.*, **80**, 6680 (1983).
7) D. M. Jerina, J. W. Daly and B. Witkop, *J. Am. Chem. Soc.*, **90**, 6523 (1968).
8) D. R. Boyd, J. W. Daly and D. M. Jerina, *Biochemistry*, **11**, 1961 (1972).
9) J. E. Ferrell, Jr. and G. H. Loew, *J. Am. Chem. Soc.*, **101**, 1385 (1979).
10) J. Daly, D. Jerina and B. Witkop, *Arch. Biochem. Biophys.*, **128**, 517 (1968).
11) *a*) Y. Ishimura, "Cytochrome P-450," ed. by R. Sato and T. Omura, Academic Press, New York, 1978, p. 209; *b*) T. Matsuura, "Oxidation Reactions with Oxygen (Sanso Sanka Hannou)," Maruzen, Tokyo, 1977, p. 41, in Japanese.
12) K. Ishida, K. Morokuma and A. Komornicki, *J. Chem. Phys.*, **66**, 2153 (1977).
13) R. C. Bingham, M. J. S. Dewar and D. H. Lo, *J. Am. Chem. Soc.*, **97**, 1285 (1975).
14) H. Tatewaki and S. Huzinaga, *J. Comp. Chem.*, **1**, 205 (1980).
15) S. Oikawa, M. Tsuda, Y. Okamura and T. Urabe, *J. Am. Chem. Soc.*, **106**, 6751 (1984).
16) P. Pulay, "Applications of Electronic Structure Theory," ed. by H. F. Schaefer III, Plenum, New York, 1977, p. 153.
17) S. Glasstone, K. J. Laidler and H. Eyring, "The Theory of Rate Process," McGraw-Hill, New York, 1941, p. 189.
18) R. H. Nobes, W. R. Rodwell, W. J. Bouma and L. Radom, *J. Am. Chem. Soc.*, **103**, 1913 (1981).
19) A. C. Hopkinson, M. H. Lien, I. G. Csizmadia and K. Yates, *Theor. Chim. Acta*, **47**, 97 (1978).
20) R. Breslow, "Organic Reaction Mechanisms," W. A. Benjamin, New York, 1966, p. 34.
21) *a*) W. B. Jakoby, "Enzymatic Basis of Detoxication," Academic Press, New York, 1980, Chapter 7; *b*) W. J. Jakoby, J. R. Bend and J. Caldwell, "Metabolic Basis of Detoxication," Academic Press, New York, 1982, p. 11.
22) E. D. Bush and W. F. Trager, *J. Med. Chem.*, **28**, 992 (1985).